

# Virtual Testing of Concrete Transport Properties

by D.P. Bentz, E.J. Garboczi, N.S. Martys, K.A. Snyder,  
W.S. Guthrie, K. Kyritsis, and N. Neithalath

Synopsis: The transport properties of concrete are critical to its field performance. Commonly encountered degradation mechanisms are dependent on ionic diffusivity, sorptivity, and permeability. In this paper, virtual testing of two of these concrete transport properties, diffusivity and permeability, will be reviewed. Virtual evaluations of ionic diffusion (and equivalently conductivity) will be presented as one example that spans the full range of applications, from computations on cement paste with micrometer resolution to a virtual rapid chloride permeability test (RCPT) that simulates the standard ASTM test method for conductivity of concrete cylinders. At the concrete scale, a hard core/soft shell (HCSS) microstructural model may be employed to estimate diffusion coefficients, while finite difference solutions of Fick's laws that incorporate sorption/reaction may be employed to evaluate remediation strategies for real world bridge decks. Virtual evaluations of permeability are dependent on a sufficient resolution of the pore sizes that are critical for flow under pressure. Two recent successful evaluations will be presented in this paper: the permeability of cement pastes (hydroceramics) cured at elevated temperatures, where transport is controlled by micrometer-sized pores, and the permeability of pervious concrete that is dominated by its coarse porosity (scale of mm). Many of the presented computational (virtual) tools are freely available over the Internet, either for direct access (remote computation) or for downloading.

**Keywords:** building technology; diffusion; durability; microstructure; permeability; transport; virtual testing.

ACI member **Dale P. Bentz** is a Chemical Engineer in the Materials and Construction Research Division, National Institute of Standards and Technology (NIST), Gaithersburg, MD. He received his BS in chemical engineering from the University of Maryland and his MS in computer and information science from Hood College. He is a member of ACI Committees 231, Properties of Concrete at Early Ages; 236, Material Science of Concrete; and 308, Curing Concrete. His research interests include experimental and computer modeling studies of the microstructure and performance of materials.

**Edward J. Garboczi**, FACI, is an NIST Fellow in the Materials and Construction Research Division, NIST. He received his BS, MS, and PhD in physics from Michigan State University. He is a member of ACI Committee 236, Material Science of Concrete. His research interests include X-ray-computed tomography of random materials; three-dimensional particle shape analysis for cement, sand, gravel, and other particulate materials, and three-dimensional computer models of the microstructure and performance of random materials.

**Nicos S. Martys** is a Physicist in the Materials and Construction Research Division, NIST. He received his PhD in physics from Johns Hopkins University in 1990. His research interests include computational modeling of transport in porous media and the rheology of suspensions.

**Kenneth A. Snyder** is a Physicist in the Materials and Construction Research Division, NIST. He received his BS in applied and engineering physics from Cornell University and his PhD in physics from the University of Maryland. His research interests include the physical chemistry of cementitious systems, and computational tools for performance prediction.

ACI member **W. Spencer Guthrie** is an Assistant Professor in the Department of Civil and Environmental Engineering, Brigham Young University, Provo, UT. He received his BS in civil and environmental engineering from Utah State University and his MS and PhD in civil engineering from Texas A&M University. His research interests include frost action in transportation materials, pavement recycling and stabilization, and condition assessment of concrete bridge decks.

**Konstantinos Kyritsis** is a PhD Student at the Institute for Materials and Processes at the University of Edinburgh, UK. He received his Diploma in materials science and engineering from the University of Ioannina, Greece. His research interests include chemistry and engineering properties of cement-based materials at elevated temperatures.

ACI Member **Narayanan Neithalath** is an Assistant Professor in the Department of Civil and Environmental Engineering at Clarkson University, Potsdam, NY. He received his MS from the Indian Institute of Technology (IIT) Madras and his PhD from Purdue University. He is a member of ACI Committees 123, Research and Current Development; 232, Fly ash and Natural Pozzolans in Concrete; 236, Material Science of Concrete; and 522, Pervious Concrete. His research interests include characterization and performance evaluation of normal and enhanced porosity cementitious systems, sensing methods for in-place performance evaluation of concretes, and hydration in modified cement systems.

## INTRODUCTION

To engineer durable concrete structures that will provide an acceptable service life, appropriate mechanical and transport properties are equally critical.<sup>1</sup> All common concrete degradation processes including corrosion of steel reinforcement, sulfate attack, alkali-silica reaction, and damage due to freezing/thawing (scaling) are strongly influenced by one or more of the following three major transport mechanisms: diffusion, permeability, and sorptivity. Thus, a viable approach to increase concrete service life is to reduce the values of these transport coefficients. Understanding the relationships between microstructure and transport can accelerate the achievement of such reductions. In this paper, approaches for obtaining an increased understanding of diffusion and permeability of cement-based materials based on computational materials science will be presented. This virtual testing of concrete properties can provide deeper insights into microstructure-property relationships and can also reduce expensive, laborious experimental testing.<sup>2</sup>

## RESEARCH SIGNIFICANCE

While computational materials science has been applied to cement-based materials for well over 20 years, it generally has focused more on fundamental scientific issues rather than real world practical scenarios. This

paper will present results that bridge this gap between computational materials science and real world applications. In addition to having immediate application to the real world problems, these results will demonstrate the powerful (and real) potential of a computational materials-science-based approach and hopefully aid in demystifying the modeling of concrete materials and performance.

## MODELING TECHNIQUES

### Microstructural Models

While the focus of this paper is on transport, a brief introduction into three different microstructural models that will be employed to provide inputs to algorithms for computing transport will be presented. The first, CEMHYD3D, is a computer model for the hydration and microstructure development of cement paste that is founded on a digital-image-based approach in which a three-dimensional computational volume is divided up into a cubic grid of voxels, where each voxel contains a single cementitious phase (starting material, water, or hydration product).<sup>3,4</sup> The hydration process is simulated by iteratively applying a set of rules to mimic dissolution, diffusion, and precipitation throughout the three-dimensional set of voxels. A typical CEMHYD3D microstructure is 100 elements on a side (or 1 million voxels in total) with a voxel dimension of 1  $\mu\text{m}$  ( $3.94 \times 10^{-5}$  in). Because the model microstructure is available as a three-dimensional digital image, it can be easily utilized as input to finite element or finite difference algorithms for computing mechanical or transport properties. At this voxel size, the CEMHYD3D model exhibits a percolation/depercolation transition for the capillary porosity at a value of about 20 %, in general agreement with experimental data for ordinary portland cement pastes.<sup>5</sup> In a percolated system, there is a continuous pathway across the microstructure within the capillary porosity. In a depercolated system, there is no such pathway within the porosity from one side of the microstructure to the opposite one.

The second microstructural model is the so-called hard core/soft shell (HCSS) model, one documented version of which is readily available from NIST.<sup>6</sup> As opposed to CEMHYD3D, HCSSModel is a continuum-based model consisting of hard impenetrable (spherical) particles, optionally surrounded by a soft shell. Originally developed to represent concrete aggregates and their surrounding interfacial transition zones (ITZ),<sup>6</sup> the model has been extended and adapted for numerous concrete applications including the mitigation of spalling of high-performance concretes via the addition of polymeric fibers,<sup>7</sup> the adaptation of the protected paste volume concept to internal curing,<sup>8</sup> and most recently the documentation of the influence of water-cement ratio ( $w/c$ ) and cement particle size distribution on particle spacing in fresh cement paste.<sup>9</sup> The model represents a three-dimensional cube of concrete (mortar or paste) and the particle size distribution for the particles is chosen to match that of the real materials. For example, models as large as a 50 mm x 50 mm x 50 mm (2 in. x 2 in. x 2 in.) cube of concrete have been created, requiring well over 1 million individual particles to adequately represent a realistic concrete aggregate size distribution. For the HCSSModel, the percolation/depercolation transition for the “bulk” phase (not contained in the hard cores or the soft shells) occurs at a volume fraction of 3 % to 4 %, as it is more difficult to disconnect the bulk phase by concentric spherical shells than it is by the random growth processes employed in the CEMHYD3D model.<sup>10,11</sup>

The third microstructural model is a general image-based reconstruction algorithm for creating a three-dimensional microstructural representation based on a two-dimensional image, as obtained using scanning electron microscopy, for example.<sup>12</sup> Assuming an isotropic material, the autocorrelation function measured on the porosity phase in the two-dimensional image is utilized to reconstruct a “representative” three-dimensional microstructure with the same porosity, surface area, and correlation as the original material. While first developed by Joshi<sup>13</sup> and then extended by Quiblier<sup>14</sup> many years ago, very recently these algorithms have found renewed applications to cement-based materials, including pervious concrete<sup>11</sup> and hydroceramics<sup>15</sup> (high temperature cements for oil and geothermal well applications) as will be demonstrated in the results to follow. For the reconstruction-based model, the percolation threshold for the “porosity” phase has been observed to be on the order of 10%, a value intermediate between the CEMHYD3D and HCSSModel values.<sup>12</sup>

### Diffusivity/Conductivity

Based on the Nernst-Einstein equation shown in equation (1), diffusion and conduction in porous microstructures containing a conductive solution can be solved using the same basic computational procedures.<sup>16</sup>

$$\frac{\sigma}{\sigma_0} = \frac{D}{D_0} \quad (1)$$

where  $\sigma$  is the conductivity of the microstructure,  $\sigma_o$  is the conductivity of the pore solution,  $D$  is the diffusivity of a specific ion in the microstructure, and  $D_o$  is the corresponding diffusion coefficient for the ion in bulk solution of identical composition. Based on this equation, an electrical analogy can be used to estimate the diffusivity of a three-dimensional cement paste microstructure such as that produced by CEMHYD3D, as shown in the top portion of Fig. 1. Adjacent voxels in the microstructure are simply connected together by resistors, where the resistance level indicates the relative conductivity (diffusivity) of the phases of the two voxels being connected. Specifically, resistors connecting together two capillary pore voxels are assigned a value of 1, while those connecting two voxels of the calcium silicate hydrate gel (C-S-H) are typically assigned a value of 250 to 400.<sup>16,17</sup> The resultant electrical network can then be solved by finite element or finite difference techniques to obtain the conductivity (diffusivity) of the complete microstructure.<sup>18</sup> Such an approach was used in the past to develop an equation for the diffusivity of tricalcium silicate pastes as a function of capillary porosity,<sup>16</sup> an approach that was later extended to cement pastes, including those with silica fume additions.<sup>17</sup>

For a continuum-based microstructure, such as one generated by the HCSSModel, applying the electrical analogy is difficult. Instead, a continuum random walker (blind ant) approach is commonly employed for estimating diffusivities (conductivities) as indicated in the middle portion of Fig. 1.<sup>6,19,20</sup> In these simulations, each blind ant carries his own watch and global positioning system (GPS) and steps randomly (and blindly) through the microstructure, with steps in a more porous ITZ taking less time than equivalent steps in the bulk cement paste, for example. After a large number (hundreds of thousands to millions) of steps, the diffusivity of the microstructure can be estimated from the mean distance squared per unit time achieved by all of the ants (Fig. 1). For a typical simulation, 10 000 ants are used. The HCSSModel provides an extremely flexible format for simulating real world variations, such as a concrete with internal curing, where the lightweight aggregates are not surrounded by the ITZs that are present around their normal weight counterparts, producing a significant reduction in the diffusion of chloride ions.<sup>21</sup>

Based on computations performed on virtual cement paste and concrete,<sup>17,20</sup> the next logical step is to proceed to virtual test procedures, such as simulating the response of a field concrete to a standard ASTM or American Association of State Highway and Transportation Officials (AASHTO) rapid chloride permeability test (RCPT) as indicated in the bottom portion of Fig. 1.<sup>22</sup> Such a virtual test has been developed by NIST and is available at <http://ciks.cbt.nist.gov/VirtualRCPT.html>. The interactive application allows the user to select their mixture proportions and testing conditions and provides predictions of the pore solution composition, its conductivity,<sup>23</sup> and ultimately the RCPT response. Features include the ability to reduce the testing time from the standard 6 h to just a few minutes, to avoid temperature effects, as suggested by Snyder et al.<sup>24</sup> in 2000 and more recently advocated by Riding et al.<sup>25</sup> An example of the predictive ability of the virtual RCPT test is provided in Fig. 2, which contrasts the experimental and virtual RCPT values<sup>22</sup> for a variety of concretes from one particular study.<sup>26</sup>

The final step in the modeling of diffusion is the prediction of chloride ion profiles obtained under realistic field exposure conditions. NIST has developed a web-based application (Computer Integrated Knowledge System-CIKS) for providing such predictions (<http://ciks.cbt.nist.gov/~bentz/millandfill/clpenmillandfill.html>).<sup>27</sup> The model is based on a one-dimensional finite difference solution for diffusion that includes chloride ion binding by the cementitious hydration products and reaction with the aluminate phases to form Friedel's salt. The user specifies the average exposure temperature and chloride loading for each month of the year, as well as a variety of mixture proportioning parameters.<sup>27</sup> Working with Brigham Young University, NIST has recently extended this application to consider real world remediation strategies such as surface treatments<sup>28</sup> and scarification and overlays (SO),<sup>29</sup> as will be presented further in the results section to follow.

### Permeability

The basic goal in computing the permeability of a material is to apply a pressure gradient across the three-dimensional microstructure and compute the resultant flow. NIST has developed and recently distributed a three-dimensional linear Stokes solver for performing this calculation for a three-dimensional microstructure consisting of pores and solids.<sup>30</sup> A finite difference solution of the linear Stokes equations for slow, incompressible, steady-state flow is utilized to determine the x, y, and z components of the fluid velocity in each porosity voxel. Once this finite difference solution converges sufficiently, the intrinsic permeability,  $k$ , of the composite three-dimensional microstructure is calculated by volume averaging the local fluid velocity (in the direction of the flow) and applying the Darcy equation:

$$u = -\frac{k}{\eta} \frac{\Delta P}{L} \quad (2)$$

where  $u$  is the average fluid velocity in the direction of the flow (x-direction) for the microstructure obtained via the Stokes solver program,  $\eta$  is the fluid viscosity, and  $L$  is the length of the sample microstructure across which an applied pressure difference of  $\Delta P$  exists.<sup>31</sup> For a given microstructure, three separate runs of the computer codes may be conducted to determine the (different) permeabilities for pressure-driven flow in the x, y, and z directions. Obviously, for permeability predictions to be accurate, the three-dimensional microstructure used as input must adequately represent the pores (sizes, connectivity, and tortuosity) that are dominating the flow paths through the material.

## RESULTS AND DISCUSSION

### Diffusivity/conductivity

Many state departments of transportation (DOTs) are concerned with the penetration of chlorides (from de-icing salts, for example) into bridge deck concretes and the resultant corrosion problems and concrete degradation. Two approaches that are often considered for remediation of existing bridge decks are the application of impermeable surface treatments to prevent ingress of future chlorides and the scarification (milling) of the existing bridge deck followed by the application of an overlay (filling), to remove the most chloride-laden portion of the concrete and replace it by a (thicker) high-performance concrete.<sup>28,29</sup> As mentioned above, the CIKS-Chloride computer model has been recently modified to simulate the effects of both of these remediation strategies.

The application of these computer models has been demonstrated in a project that considered differences in predicted performance for various cover depths for bridge decks with and without stay-in-place metal forms (SIPMFs).<sup>28,29</sup> Relevant chloride ion diffusion coefficients were determined from chloride-ion profile measurements obtained on specimens from 12 existing concrete bridge decks (six without SIPMFs and six with SIPMFs). The CIKS system was then employed to simulate chloride concentrations at the (variable) depth of cover as a function of the exposure age and the time of application of a given remediation strategy. Example results are shown in Figures 3 and 4 for the case of a 50 mm (2 in.) concrete cover. When SIPMFs are employed, higher diffusion coefficients are measured, due to the increased saturation level of the concrete. This requires the remediation strategies to be employed at earlier times to provide the same performance. Table 1 summarizes the latest time at which successful remediation can be achieved with the performance criteria that the chloride concentration at the level of the top layer of reinforcement (cover depth) does not exceed 1.18 kg/m<sup>3</sup> (2 lb/yd<sup>3</sup>). Because the scarification and overlay treatment actually removes a portion of the chlorides (in the removed top layer of the concrete), treatment can be slightly delayed when this more severe (and expensive) remediation strategy is employed. However, the differences between treatments are far outweighed by the differences in deck type due to the increase in chloride ion diffusion coefficients for decks with SIPMFs compared to those without SIPMF. This study thus emphasizes the criticality of producing a concrete with a low chloride ion diffusivity.

### Permeability

Originally, the permeability computation codes were developed with the hopes of computing permeabilities as a function of degree of hydration for cement paste microstructures. While the predictions for fresh cement pastes were reasonable, experimental permeabilities fell dramatically as the capillary pores depercolated during hydration and the digital-image-based cement paste microstructural model was not able to adequately resolve a wide enough range of pores sizes to provide reasonable permeability predictions. The permeability codes then remained dormant for a number of years until recently when two new applications were found: cement pastes cured at elevated temperatures (hydroceramics) and pervious concrete.

In deep oil and geothermal well cementing applications, hydration occurs at vastly elevated temperatures, as the wells have typical working temperatures in the range of 200 to 350 °C (392 to 662 °F).<sup>15</sup> This requires the utilization of special cements and leads to the formation of a variety of hydration products not typically encountered for room temperature hydration.<sup>15</sup> In addition, the porosities of these materials are generally higher and the pore sizes larger than those in a well hydrated ordinary portland cement. Thus, application of the permeability computation procedures to these hydroceramic materials was of interest. The general procedure employed in reference 15 is summarized in Fig. 5. Starting from a two-dimensional scanning electron microscopy (SEM) image, a binary (pore/solid) image is obtained and analyzed by determining the two-dimensional correlation function for the porosity phase. This correlation function and the experimentally measured porosity for the material (values in the range of 25% to 40%) are then used to reconstruct a three-dimensional representation of the microstructure based on the procedures described above. The permeability computation code is then employed to compute a fluid permeability for the reconstructed microstructure.



Experimental and computational results are compared in Figure 6 for hydroceramics cured at 200°C (392°F) and containing either alumina or silica additions. While the alumina creates a more porous and permeable microstructure, the silica produces a denser microstructure with a dramatically reduced permeability. For both silica and alumina additions, the experimental trends are well captured by the estimates provided by the computational procedures. Further, the predictions are observed to be reasonably accurate for permeabilities spanning four orders of magnitude.

A second application where permeability is controlled by pores in a very limited size range is that of pervious concrete. Pervious concrete is basically produced by removing the fine aggregate fraction from a concrete mixture, producing a concrete with enhanced porosity and a set of connected pores that are up to several millimeters in size. In this case, an optical microscope can be utilized to capture a two-dimensional image of the porosity of the pervious concrete. The same two-dimensional image to three-dimensional microstructure algorithms can then be employed as shown in Figure 5. Figure 7 provides an overview of the process for a pervious concrete, along with a graph comparing previously obtained experimental and model permeability values. Once again, the predictions provided by the reconstruction/computation algorithms are in reasonable agreement with the experimental values compiled from three different sources.<sup>32-34</sup> Conversely, as shown in the graph in Figure 7, model predictions generated based on a version of the HCSSModel produced permeabilities that were well above those measured experimentally, most likely due to that models much lower percolation threshold as mentioned earlier. In addition to permeability, the reconstructed three-dimensional microstructures of the pervious concrete can also be analyzed to assess other issues such as the potentials for clogging and freezing/thawing damage.<sup>11</sup>

## SUMMARY AND PROSPECTUS

Successful applications of virtual testing of transport properties have been demonstrated for both diffusion and permeability. In the case of diffusion, a multi-scale approach allows modeling of transport from the nanoscale (C-S-H) to the macroscale (bridge decks). Finite difference, finite element, and random walk computational methods are valuable techniques for transforming microstructural representations into quantitative diffusion coefficients. Such an approach can be further extended to consider changes in transport properties due to material damage including leaching<sup>35</sup> and tensile cracking.<sup>36</sup> In the case of permeability, a 3-D microstructure reconstruction method has been paired with a Stokes solver to provide a quantitative virtual permeability test. Predictions for porous hydroceramics and pervious concrete agree well with experimental measurements. In both of these cases, pore structures of materials with nominally 20% to 30% porosity are well captured by the reconstruction method, whose inherent percolation threshold of around 10% can sometimes limit the accuracy of predictions at lower porosity values.<sup>12</sup>

Virtual testing of concrete transport properties aids in the development of fundamental microstructure/property relationships, such as those between transport coefficients and porosity (Fig. 7) or other microstructural characteristics. Additionally, virtual testing has the potential to be applied to a wide variety of “what if” field scenarios to optimize mitigation and remediation strategies, as demonstrated for remediation of chloride-contaminated bridge deck concretes (Fig. 3 and 4). The various models described in this paper and their locations on the Internet are summarized in Table 2. All are freely available for execution and/or downloading; documentation in the form of user manuals or accompanying technical articles is also provided.

## REFERENCES

1. B. Mobasher and J. Skalny, eds., *Transport Properties and Concrete Quality*, Materials Science of Concrete Special Volume, John Wiley & Sons, Inc., Hoboken, NJ, 2007.
2. Bentz, D.P.; Garboczi, E.J.; Bullard, J.W.; Ferraris, C.F.; Martys, N.S.; and Stutzman, P.E., “Virtual Testing of Cement and Concrete,” ASTM STP 169D, *Significance of Tests and Properties of Concrete and Concrete-Making Materials*, J.F. Lamond and J.H. Pielert, eds., ASTM International, West Conshohocken, PA, 2006, pp. 38-50.
3. Bentz, D.P., “Three-Dimensional Computer Simulation of Cement Hydration and Microstructure Development,” *Journal of the American Ceramic Society*, V. 80, No. 1, 1997, pp. 3-21.
4. Bentz, D.P., “CEMHYD3D: A Three-Dimensional Cement Hydration and Microstructure Development Modeling Package,” Version 3.0, NISTIR 7232, U.S. Department of Commerce, June 2005.
5. Bentz, D.P., “Capillary Porosity Depercolation/Repercolation in Hydrating Cement Pastes via Low Temperature Calorimetry Measurements and CEMHYD3D Modeling,” *Journal of the American Ceramic Society*, V. 89, No. 8, 2006, pp. 2606-2611.
6. Bentz, D.P.; Garboczi, E.J.; and Snyder, K.A., “A Hard Core/Soft Shell Microstructural Model for Studying Percolation and Transport in Three-Dimensional Composite Media,” NISTIR 6265, U.S. Department of Commerce, Jan. 1999.

7. Bentz, D.P., "Fibers, Percolation, and Spalling of High Performance Concrete," *ACI Materials Journal*, V. 97, No. 3, May-June 2000, pp. 351-359.
8. Bentz, D.P., and Snyder, K.A., "Protected Paste Volume in Concrete: Extension to Internal Curing using Saturated Lightweight Fine Aggregates," *Cement and Concrete Research*, V. 29, No. 11, 1999, pp. 1863-1867.
9. Bentz, D.P., and Aitcin P.C., "The Hidden Meaning of Water-to-Cement Ratio," *Concrete International*, V. 30, No. 5, May 2008, pp. 51-54.
10. Elam, W.T.; Kerstein, A.R.; and Rehr, J.J., "Critical Properties of Void Percolation Problem for Spheres," *Physical Review Letters*, V. 52, No. 17, 1984, pp. 1516-1519.
11. Bentz, D.P., "Virtual Pervious Concrete: Microstructure, Porosity Percolation, and Permeability Predictions," *ACI Materials Journal*, V. 105, No. 3, May-June 2008, pp. 297-301.
12. Bentz, D.P., and Martys, N.S., "Hydraulic Radius and Transport in Reconstructed Model Three-Dimensional Porous Media," *Transport in Porous Media*, V. 17, No. 3, 1995, pp. 221-238.
13. Joshi, M., "A Class of Stochastic Models for Porous Media," PhD thesis, University of Kansas, Lawrence, KS, 1974.
14. Quiblier, J.A., "A New Three-Dimensional Modeling Technique for Studying Porous Media," *Journal of Colloidal and Interface Science*, V. 98, No. 1, 1984, pp. 84-102.
15. Kyritsis, K.; Hall, C.; Bentz, D.P.; Meller, N.; and Wilson, M.A., "Relationship between Engineering Properties, Mineralogy and Microstructure in Cement-Based Hydroceramic Materials Cured at 200°C to 350°C," submitted to *Journal of the American Ceramic Society*, V. 92, No. 3, 2009, pp. 694-701.
16. Garboczi, E.J., and Bentz, D.P., "Computer Simulation of the Diffusivity of Cement-Based Materials," *Journal of Materials Science*, V. 27, 1992, pp. 2083-2092.
17. Bentz, D.P.; Jensen, O.M.; Coats, A.M.; and Glasser, F.P., "Influence of Silica Fume on Diffusivity in Cement-Based Materials—I: Experimental and Computer Modeling Studies on Cement Pastes," *Cement and Concrete Research*, V. 30, No. 6, 2000, pp. 953-962.
18. Garboczi, E.J., "Finite Element and Finite Difference Programs for Computing the Linear Electrical and Elastic Properties of Digital Images of Random Materials," NISTIR 6269, U.S. Department of Commerce, Dec. 1998.
19. Schwartz, L.M.; Garboczi, E.J.; and Bentz, D.P., "Interfacial Transport in Porous Media: Application to D.C. Electrical Conductivity of Mortars," *Journal of Applied Physics*, V. 78, No. 10, 1995, pp. 5898-5908.
20. Bentz, D.P.; Garboczi, E.J.; and Lagergren, E.S., "Multi-Scale Microstructural Modelling of Concrete Diffusivity: Identification of Significant Variables," *Cement, Concrete, and Aggregates*, V. 20, No. 1, 1998, pp. 129-139.
21. Bentz, D.P., "Influence of Internal Curing Using Lightweight Aggregates on Interfacial Transition Zone Percolation and Chloride Ingress in Mortars," *Cement and Concrete Composites*, V. 31, No. 5, May 2009, pp. 285-289.
22. Bentz, D.P., "A Virtual Rapid Chloride Permeability Test," *Cement and Concrete Composites*, V. 29, No. 10, 2007, pp. 723-731.
23. Snyder, K.A.; Feng, X.; Keen, B.D.; Mason, T.O., "Estimating the Electrical Conductivity of Cement Paste Pore Solutions from OH<sup>-</sup>, K<sup>+</sup>, and Na<sup>+</sup> Concentrations," *Cement and Concrete Research*, V. 33, No. 6, 2003, pp. 793-798.
24. Snyder, K.A.; Ferraris, C.F.; Martys, N.S.; and Garboczi, E.J., "Using Impedance Spectroscopy to Assess the Viability of the Rapid Chloride Test for Determining Concrete Conductivity," *Journal of Research of the National Institute of Standards and Technology*, V. 105, No. 4, 2000, pp. 497-509.
25. Riding, K.A.; Poole, J.L.; Schindler, A.K.; Juenger, M.C.G.; and Folliard, K.J., "Simplified Concrete Resistivity and Rapid Chloride Permeability Test Method," *ACI Materials Journal*, V. 105, No. 4, July-Aug. 2008, pp. 390-394.
26. Simon, M.J.; Lagergren, E.S.; and Snyder, K.A., "Concrete Mixture Optimization Using Statistical Mixture Design Methods," *Proceedings of the PCI/FHWA International Symposium on High Performance Concrete*, 1997, pp. 230-244.
27. Bentz, D.P.; Clifton, J.R.; and Snyder, K.A., "A Prototype Computer-Integrated Knowledge System: Predicting Service Life of Chloride-Exposed Steel-Reinforced Concrete," *Concrete International*, V. 18, No. 12, Dec. 1996, pp. 42-47.
28. Birdsall, A.W.; Guthrie, W.S.; and Bentz, D.P., "Effects of Initial Surface Treatment Timing on Chloride Concentrations in Concrete Bridge Decks," *Transportation Research Record: Journal of the Transportation Research Board*, No. 2028, Design of Structures 2007, Transportation Research Board, National Research Council, Washington, DC, 2007, pp. 103-110.
29. Nolan, C.D., "Effect of Initial Scarification and Overlay Treatment Timing on Chloride Concentrations in Concrete Bridge Decks," MS thesis, Brigham Young University, 2008.
30. Bentz, D.P., and Martys, N.S., "A Stokes Permeability Solver for Three-Dimensional Porous Media," NISTIR 7416, U.S. Department of Commerce, Apr. 2007.
31. Martys, N.S.; Torquato, S.; and Bentz, D.P., "Universal Scaling of Fluid Permeability for Sphere Packings," *Physical Review E*, V. 50, No. 1, 1994, pp. 403-408.
32. Montes, F., and Haselbach, L., "Measuring Hydraulic Conductivity on Pervious Concrete," *Environmental Engineering Science*, V. 23, No. 6, 2006, pp. 960-969.
33. Neithalath, N.; Weiss, J.; and Olek, J., "Characterizing Enhanced Porosity Concrete Using Electrical Impedance to Predict Acoustic and Hydraulic Performance," *Cement and Concrete Research*, V. 36, No. 11, 2006, pp. 2074-2085.
34. Schaefer, V.R.; Wang, K.; Suleiman, M.T.; and Kevern, J.T., "Mix Design Development for Pervious Concrete in Cold Weather Climates," *Final Report*, Report 2006-1, National Concrete Pavement Technology Center, Feb. 2006.

35. Bentz, D.P., and Garboczi, E.J., "Modeling the Leaching of Calcium Hydroxide from Cement Paste: Effects on Pore Space Percolation and Diffusivity," *Materials and Structures*, V. 25, 1992, pp. 523-533.
36. Kamali-Bernard, S., and Bernard, F., "Effect of Tensile Cracking on Diffusivity of Mortar: 3D Numerical Modeling," *Computational Materials Science*, 2009, in press.

**Table 1—Latest treatment times versus bridge deck type and remediation strategy**

Bridge deck type	Treatment type	Latest treatment time
SIPMF	Surface	1 year
No SIPMF	Surface	5 years
SIPMF	Scarification and overlay	2 years
No SIPMF	Scarification and overlay	6 years

**Table 2—NIST models for virtual testing (available for remote execution or downloading)**

Model	Description/Purpose	Download location or web page address
CEMHYD3D	Cement hydration (version 3.0)	<a href="ftp://ftp.nist.gov/pub/bfrl/bentz/CEMHYD3D/version30">ftp://ftp.nist.gov/pub/bfrl/bentz/CEMHYD3D/version30</a>
HCSSModel	Hard core/soft shell 3-D microstructural model	<a href="http://ciks.cbt.nist.gov/cmml.html">http://ciks.cbt.nist.gov/cmml.html</a>
3-D Reconstruction	Correlation-based transformation from 2-D image to 3-D microstructure	<a href="ftp://ftp.nist.gov/pub/bfrl/bentz/permsolver/">ftp://ftp.nist.gov/pub/bfrl/bentz/permsolver/</a>
VirtualRCPT	Virtual RCPT test	<a href="http://ciks.cbt.nist.gov/VirtualRCPT.html">http://ciks.cbt.nist.gov/VirtualRCPT.html</a>
CIKS-Chloride	Chloride penetration simulation including surface treatment and/or scarification and overlay	<a href="http://ciks.cbt.nist.gov/~bentz/millandfill/clpenmillandfill.html">http://ciks.cbt.nist.gov/~bentz/millandfill/clpenmillandfill.html</a>
Permsolver	3-D Stokes solver for permeability	<a href="ftp://ftp.nist.gov/pub/bfrl/bentz/permsolver/">ftp://ftp.nist.gov/pub/bfrl/bentz/permsolver/</a>

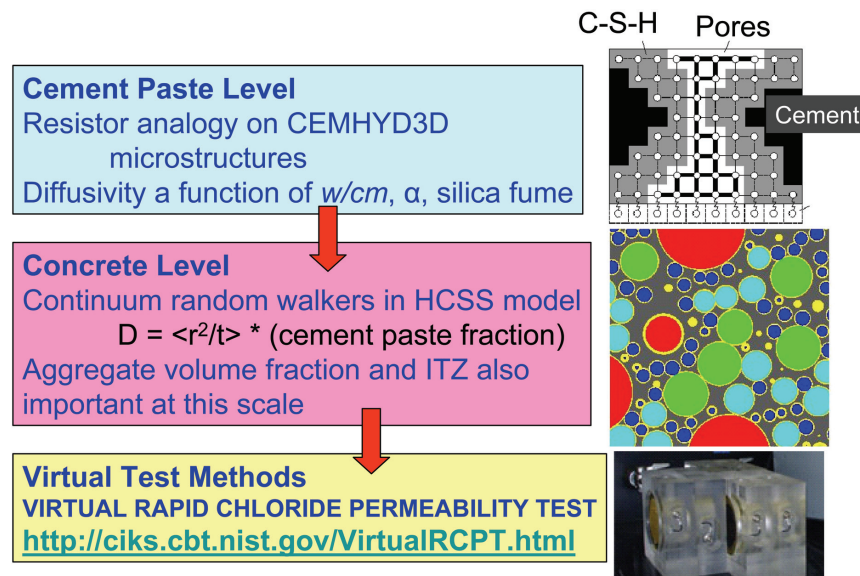


Fig. 1—Summary of multi-scale modeling of conductivity/diffusivity in cement-based materials.



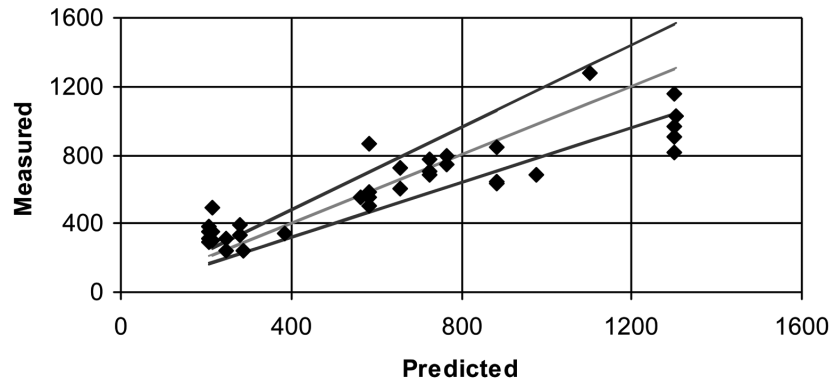


Fig. 2—Measured versus predicted (virtual) RCPT test results.<sup>22</sup> Experimental data taken from Reference 26. Gray line indicates line of equality, and dark lines indicate  $\pm 20\%$  of the measured values.

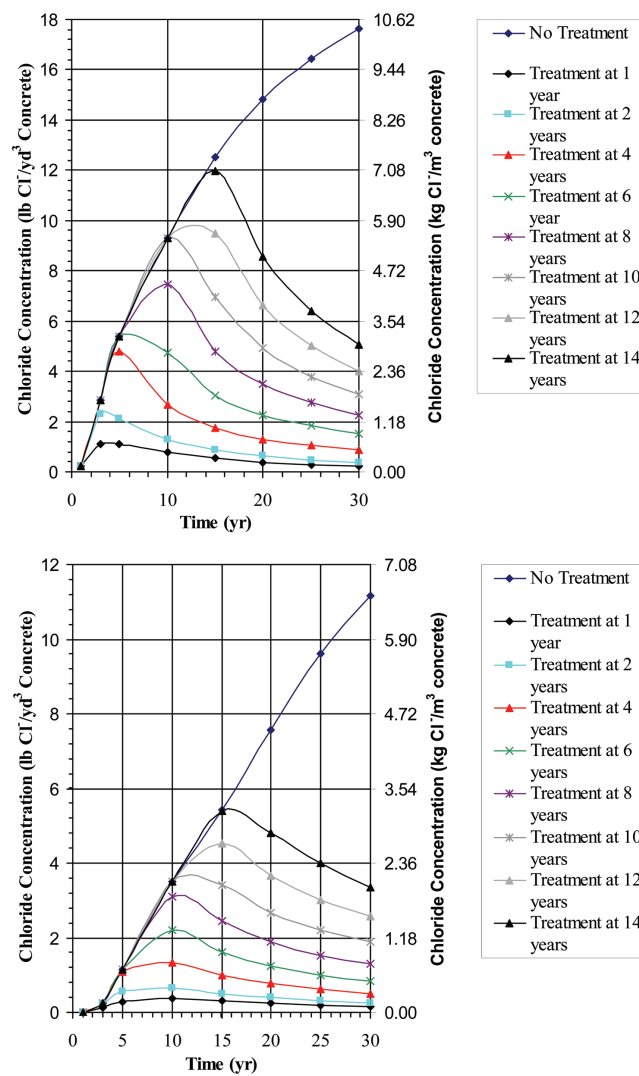


Fig. 3—Comparison of simulated chloride concentrations of decks with (top) and without (bottom) SIPMFs at 50 mm (2 in.) cover depth as a function of time of application of surface treatment.<sup>28</sup>

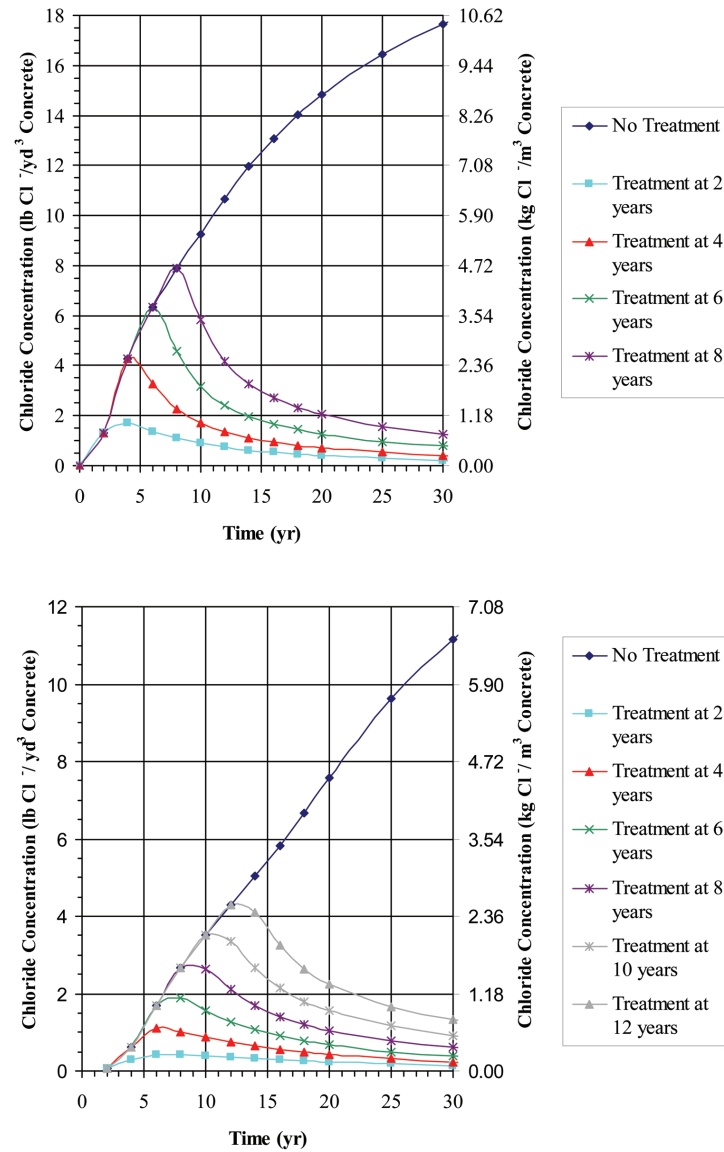


Fig. 4—Comparison of simulated chloride concentrations of decks with (top) and without (bottom) SIPMFs at 50 mm (2 in.) cover depth as a function of timing of a 12.7 mm (0.5 in.) scarification and 38 mm (1.5 in.) overlay treatment.<sup>29</sup>

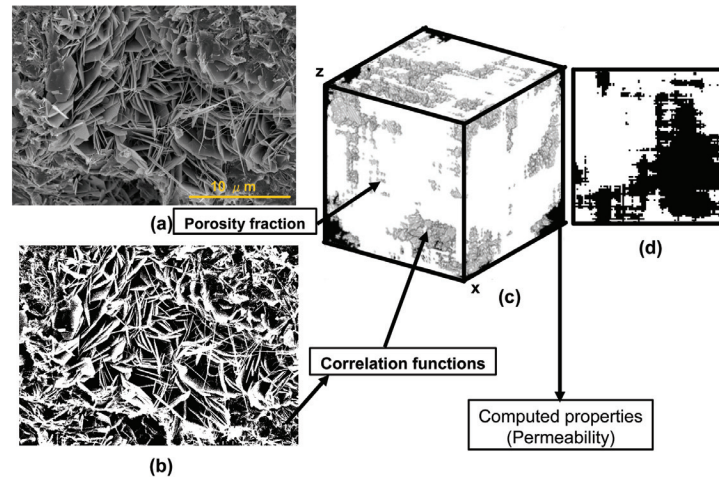


Fig. 5—Illustration of the process of creating a three-dimensional microstructure for subsequent computation of permeability<sup>15</sup>: (a) SEM image showing hexagonal crystals of truscottite. The needle shaped crystals are of xonotlite. Sample cured at 350°C (662°F) containing 40% by mass of silica flour; (b) binary image used to extract the correlation functions for the 3-D reconstruction; (c) reconstructed three-dimensional microstructure (100 pixels x 100 pixels x 100 pixels) for which permeability is computed; and (d) slice of the reconstructed three-dimensional microstructure.

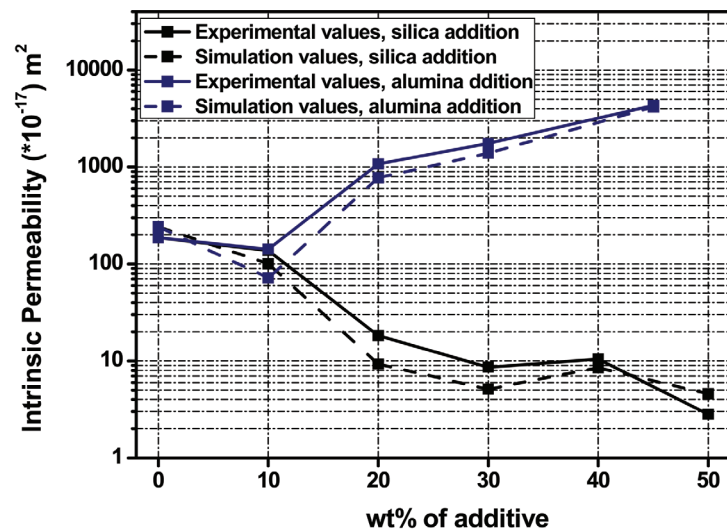


Fig. 6—Comparison of experimental and simulation values of intrinsic permeability with silica or alumina additions in hydroceramic samples.<sup>15</sup> (Note: 1  $m^2$  = 10.76  $ft^2$ .)

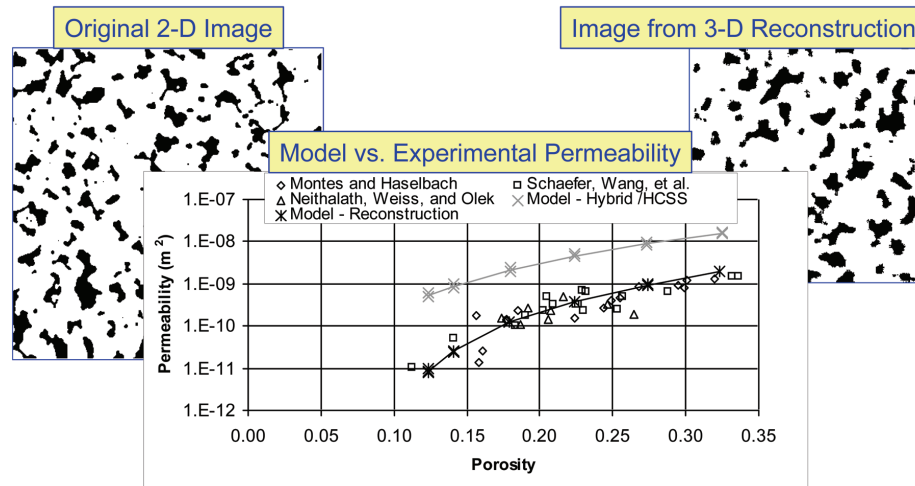


Fig. 7—Comparison of experimental and simulation values for intrinsic permeability for pervious concretes.<sup>11</sup> Original image is 63 by 63 mm (2.5 by 2.5 in.). Experimental values were extracted from the references listed in the legend.<sup>32-34</sup> (Note:  $1\text{ m}^2 = 10.76\text{ ft}^2$ .)